

Novel Corrections to the Momentum Sum Rule for Nuclear Structure Functions

Stanley J. Brodsky^a, Valery E. Lyubovitskij^{b,c,d,*}, Ivan Schmidt^c

^a*SLAC National Accelerator Laboratory, Stanford University, Stanford, CA 94309, USA*

^b*Institut für Theoretische Physik, Universität Tübingen, Kepler Center for Astro and Particle Physics,
Auf der Morgenstelle 14, D-72076 Tübingen, Germany*

^c*Departamento de Física y Centro Científico Tecnológico de Valparaíso-CCTVal,
Universidad Técnica Federico Santa María, Casilla 110-V, Valparaíso, Chile*

^d*Millennium Institute for Subatomic Physics at the High-Energy Frontier (SAPHIR) of ANID,
Fernández Concha 700, Santiago, Chile*

Abstract

We address novel features of deep inelastic lepton scattering on nuclei at small Bjorken variable x_{Bj} . In this regime the lepton-nuclear cross section involves the interference between the standard lepton-quark scattering amplitude for the deep inelastic scattering (DIS) process on a single nucleon and a two-step process where diffractive scattering on a first nucleon combines with the amplitude for DIS on a second nucleon. The phases associated with the t -channel exchanges to the diffractive amplitude can produce either a destructive or constructive quantum-mechanical interference of the one-step and two-step amplitudes. This provides a mechanism regulating the respective amounts of shadowing suppression and anti-shadowing enhancement at low x_{Bj} . Furthermore, the standard leading-twist operator product and handbag diagram analyses of the forward virtual Compton amplitude on the nucleus are inapplicable, barring a conventional probabilistic interpretation. A main observable consequence is the impossibility of extracting momentum and spin sum rules from nuclear structure functions. We present numerical predictions supporting this picture and test them against DIS neutrino-nucleus and charged-lepton-nucleus scattering data.

Keywords:

Deep inelastic scattering, diffractive deep inelastic scattering, parton distribution functions, nuclear structure functions, momentum sum rules, operator expansion

*Corresponding author at: Institut für Theoretische Physik, Universität Tübingen, Kepler Center for Astro and Particle Physics, Auf der Morgenstelle 14, D-72076 Tübingen, Germany

Email addresses: sjbth@slac.stanford.edu (Stanley J. Brodsky), valeri.lyubovitskij@uni-tuebingen.de (Valery E. Lyubovitskij), ivan.schmidt@usm.cl (Ivan Schmidt)

Deep inelastic scattering (DIS) processes measure the proton structure functions, which can be interpreted at leading twist in QCD in terms of the probability, $q(x, Q^2)$, for finding a quark with a given light-front momentum fraction $x = \frac{k^+}{p^+}$ of the proton's light-front momentum $p^+ = p^0 + p^z$, at large spacelike four-momentum transfer, $Q^2 = -q^2$. Longitudinal fraction variable x is identified with Bjorken variable x_{Bj} and is expressed in terms of invariants as $x = x_{Bj} = Q^2/(2pq)$ with p being the proton four-momentum.

Perturbative QCD radiative processes generate the Q^2 evolution of $q(x, Q^2)$, consistent with the renormalization group. The Mellin moments of the structure functions are in one-to-one correspondence with the matrix elements of the operators in the operator product expansion for the forward virtual Compton amplitude $\gamma^* p \rightarrow \gamma^* p$. The second Mellin moment, in particular, gives the momentum sum rule (MSR),

$$M_2 = \int_0^1 dx x \left[\sum_q [q(x, Q^2) + \bar{q}(x, Q^2)] + g(x, Q^2) \right] = 1, \quad (1)$$

where $\sum_q (q + \bar{q})$ is the flavor-singlet contribution and g is the gluon distribution. Notice that the anomalous dimensions for M_2 is equal to 0 so that the Q^2 dependence of the quark and gluon coefficient functions is guaranteed to cancel in the sum of the two contributions. One should stress that the gluon momentum fraction in nucleons has to be corrected because of the diffractive contribution to DIS.

The parton distributions in Eq. (1) are derived by Fourier transforming the quark-quark correlation function, written as a function of the light-cone variable, z^- , with the quark/gluon fields evaluated at light front coordinates, $z_{in}^- = 0$, and $z_{out}^- = z^-$ [1]. In the standard QCD scenario we can take the limit $z^- \rightarrow 0$, obtaining the integral definitions of the moments in Eq. (1), where the product of the two electroweak currents, $j^\mu(z)$ and $j^\nu(0)$ (where $j^\mu(z) = \bar{\psi}(z)\Gamma^\mu\psi(z)$ and $\Gamma^\mu = \gamma^\mu$ or $\gamma^\mu\gamma^5$), acting on an uninterrupted quark propagator is replaced by a local operator. This defines the factorized handbag diagram where the real phase of the resulting DIS amplitude – the virtual Compton scattering amplitude $\gamma^* p \rightarrow \gamma^* p$ in the forward limit – reflects the real phase of the stable target hadron's wavefunction. Similar results are obtained for $\bar{q}(x)$ and $g(x)$.

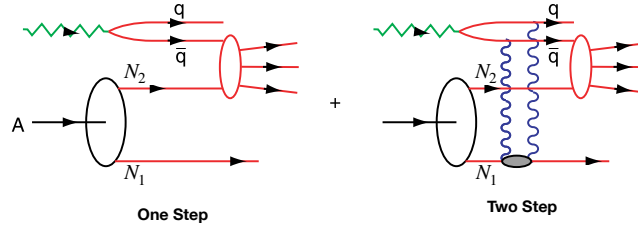


Figure 1. One-step (left panel) and two-step (right panel) scattering amplitudes in DIS on a nucleus A.

In this Letter we argue that the QCD standard picture breaks down in a nucleus because the forward virtual Compton scattering amplitude for the process, $\gamma^*(Q^2)A \rightarrow \gamma^*(Q^2)A$, includes at low x a leading-twist contribution from the interference between the one-step and two-step amplitudes shown in Fig. 1. In particular, the initial scattering in the two-step amplitude on the front-face nucleon N_1 is Diffractive DIS (DDIS): $\gamma^* N_1 \rightarrow [q\bar{q}]N_1'$ which leaves N_1 intact. The propagating vector $(q\bar{q})$ system then interacts inelastically on N_2 : $[q\bar{q}] + N_2 \rightarrow X$. The two step amplitude interferes with the one-step amplitude $\gamma^* + N_2 \rightarrow X$ on N_2 . The interior nucleon N_2 sees two fluxes, the virtual photon γ^* and the secondary beam $(q\bar{q})$ generated by DDIS on N_1 . In effect, nucleon N_1 “shadows” N_2 . The smooth limit, $z^- \rightarrow 0$, is inapplicable in this case since the currents can act on different nucleons. Because of this type of quantum interference between the scattering amplitudes from two-step and one-step amplitudes in nuclei, incoherent scattering on a single quark is ruled out by definition, as well as its probabilistic interpretation and the validity of the MSR, Eq. (1). The contribution to doubly virtual Compton scattering on a nucleus $\gamma^* A \rightarrow \gamma^* A$ from the interference of two-

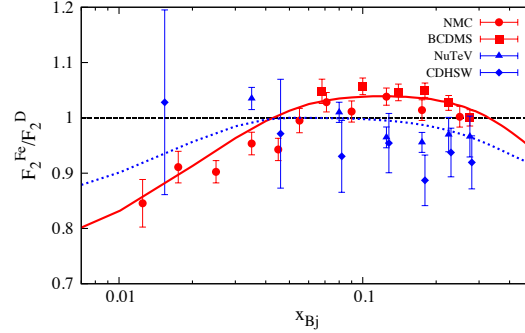


Figure 2. Comparison of the ratio of iron to deuteron nuclear structure functions measured in the DIS neutrino-nucleus scattering (NuTeV [3], CDHSW [4]), and muon-nucleus scattering (BCDMS [5] and NMC [6, 7]). All data are displayed in the online Durham HepData Project Database [8]. Anti-shadowing is absent in the neutrino charged current data.

step and one-step amplitudes cannot be reduced to a handbag amplitude where two currents interact on an interrupted quark propagator.

The picture presented here is consistent with the analysis of shadowing in the dipole formalism. The dipole analysis uses the target rest frame where two length scales are important. One is the coherence length ($\approx 1/\sqrt{Q^2}$), which has to be much larger than the inter-nucleon separation, and the other is the $\bar{q}q$ transverse separation, which has to be large enough so that the virtual photon interacts with a sizable cross section. These large length scales conflict with the applicability of the OPE in nuclear shadowing processes, and therefore, on the validity of the nuclear MSR [2].

The breaking of the MSR, according to the quantum interference interpretation that we suggest here, and the flavor dependence of the t -channel exchanges in the diffractive process, also provide a much sought-for explanation of one of the most surprising results of the NuTeV measurement [3] of nuclear structure functions in the DIS charged-current reactions $\nu A \rightarrow \mu X$, concerning the absence of anti-shadowing in the domain $0.1 < x_{Bj} < 0.2$ (see Fig. 2). NuTeV's initial measurement was further substantiated by the global analysis conducted by nCTEQ [9] where, based on the fully correlated covariant error matrix provided in [3], it is shown that the tension between the νFe and μFe data does not allow for a “compromise” fit including both sets. A similar conclusion has also been reached in the more recent experimental analyses of Refs. [10, 11, 12], as well as in Ref. [13], where following an accurate analysis of the Q^2 dependence of the different data sets, the nuclear parton distribution functions (PDFs) measured in the DIS neutrino reactions is shown to have no anti-shadowing enhancement and is thus distinctly different from the corresponding PDF measured in the charged lepton DIS (see Fig. 2). More quantitative analyses are in currently in progress to better constrain the shadowing and anti-shadowing regions.

The striking difference between neutrino vs. charged lepton DIS measurements is in direct conflict with the conventional expectation that the quark and gluon distributions of the nucleus are universal properties of the nuclear eigenstate and are thus process independent (see discussion in [14]). Moreover, the NuTeV measurement contradicts the expectation that anti-shadowing $\frac{d\sigma_A}{Ad\sigma_N} < 1$ which is observed in the domain $0.1 < x_{Bj} < 0.2$ in order to restore the MSR [15].

Understanding the workings of low x PDFs in nuclei and their impact on the MSR is of the utmost importance, especially as more precise measurements on nuclear PDFs will be made available at the upcoming Electron Ion Collider (EIC).

We describe a scenario by which both shadowing and anti-shadowing originate as Glauber phenomena involving the constructive vs. destructive interference of two-step and one-step amplitudes illustrated in Fig. 1 of Ref. [16]. The first step of the two-step amplitude involves leading-twist DDIS on a front-face nucleon N_1 , which leaves the nucleon intact. DDIS underly the shadowing and antishadowing of nucleus structure functions through the two-step amplitude. DDIS in $\gamma^* N \rightarrow NX$ reactions has been observed to satisfy Bjorken scaling, and approximately 10% of high energy DIS events are diffractive [17, 18]. In the Regge theory of strong interactions diffraction occurs through the exchange of either a Pomeron or a Reggeon trajectory. In quantum chromodynamics (QCD), the Pomeron and

the Reggeon correspond to two gluon and to quark-antiquark color-singlet exchanges, respectively. The diffractive process is leading twist and it, therefore, displays Bjorken scaling.

The second step of the two-step amplitude is a standard inelastic scattering on a second nucleon, N_2 , producing a final state X . The interference of the two-step amplitude with the DIS event on nucleon N_2 shown in Fig. 1 (bottom panel) can produce shadowing or anti-shadowing of the nuclear PDF depending on the phase of the DDIS amplitude.

Unlike the handbag diagram, the phase of the deeply virtual amplitude arising from the Glauber interference amplitudes is always complex. In a nucleus we define the ratio of structure functions, $R_A = F_2^A / A F_2^N$, in terms of the imaginary part of the forward quark-nucleon scattering amplitude, T_{qN} as,

$$R_A(x, Q^2) = \frac{\int ds dk_T^2 \Im T_{qA}(s, k^2)}{A \int ds dk_T^2 \Im T_{qN}(s, k^2)} \quad (2)$$

with T_{qA} given in Glauber theory as follows [19, 20],

$$\begin{aligned} T_{qA} &= \sum_{j=1}^A \frac{1}{j} \binom{A}{j} T_{qN} \left(\frac{i T_{qN}}{4\pi p_{CM} s^{1/2} (R^2 + 2b)} \right)^{j-1} \\ &\approx A T_{qN} \left(1 + \frac{i(A-1) T_{qN}}{8\pi p_{CM} s^{1/2} (R^2 + 2b)} \right) \end{aligned} \quad (3)$$

where $s = (k + p)^2 \approx 1/x$ is the parton-proton center of mass energy squared, k^2 is the quark virtuality, k_T^2 is the quark transverse momentum squared, related linearly to k^2 , p_{CM} is the quark-proton center of mass momentum, $R = 1.12 A^{1/3}$ fm is the nuclear radius, $b = 10 \text{ GeV}^{-2}$ is the parameter defining the slope of the non forward amplitude, $T_{qN} = T_{qN}(s, k^2) \exp(-bq_T^2)$. T_{qN} describes Regge exchanges with all allowed J^{PC} quantum numbers. We used a form containing the two essential contributions from Pomeron (β_1) and Reggeon ($\beta_{1/2}$) exchanges, respectively given by [19, 20],

$$T_{qN} \approx \sigma \left(i s \beta_1 (-k^2) + \frac{1}{\sqrt{2}} (1 - i) s^{1/2} \beta_{1/2} (-k^2) \right). \quad (4)$$

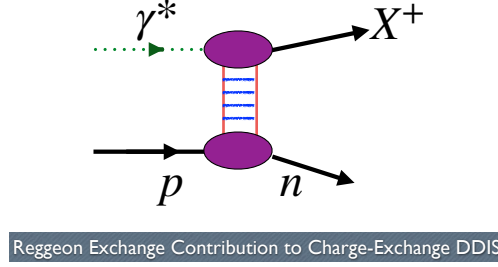
From this expression one can clearly see that multiplying by the phase i from the propagating intermediate state, or Glauber cut, the relative phase of the two-step amplitude, $\propto i \times i$ is destructive if the diffractive component is due to Pomeron exchange thus producing shadowing. On the contrary, Reggeon exchanges enable constructive interference, $\propto i \times (-i)$, thus anti-shadowing. Notice that due to the inverse proportionality of s and x , the anti-shadowing term is predicted to appear at larger values of x . The resulting effect from the constructive interference appears in the $0.1 < x_{Bj} < 0.2$, domain of the nuclear PDF. Notice that the exchange of the same Reggeon also leads to the Kutik-Weisskopf prediction: $F_2^p(x, Q^2) - F_2^n(x, Q^2) \propto \sqrt{x}$ (this result is consistent with recent evaluations in Refs. [21, 22]).

Eqs. (3) and (4) describe the situation in Fig. 1 where N_1 is the front-face nucleon and N_2 is an interior nucleon. In the one-step process only N_2 interacts via Pomeron exchange, while N_1 does not. One can see that if the scattering on N_1 is, *e.g.*, via Pomeron exchange, and both amplitudes have different phases, diminishing the \bar{q} flux that reaches N_2 . The interior nucleon, N_2 , thus sees two fluxes – the incident virtual photon γ^* and the $q\bar{q}$ vector system, V^0 (grey blob in the bottom rungs in Fig. 2), produced from DDIS on N_1 . The relative phase of the one-step and two-step amplitudes is the critical factor of i from the Glauber cut times the phase of Pomeron exchange in DDIS. The destructive interference is why N_2 does not see the full flux – it is shadowed by N_1 . Thus shadowing of the nuclear PDF is due to additional physical, causal events within the nucleus. Being defined by interference terms, the MSR can fail for the nuclear PDFs: as shown in our numerical evaluation in Fig. 2, shadowing and anti-shadowing do not need to compensate each other to restore the MSR.

Thus unlike shadowing, anti-shadowing from Reggeon exchange is flavor specific; *i.e.*, each quark and anti-quark will have distinctly different constructive interference patterns. The flavor dependence of anti-shadowing explains why its amount varies in electron (neutral electromagnetic current) vs. neutrino (charged weak current) DIS reactions, based on the flavor composition of the DIS isoscalar nuclear and nucleon structure functions,

$$\frac{1}{2x} F_2^{\nu N(A)} = d_{N(A)} + s_{N(A)} + \bar{u}_{N(A)} + \bar{c}_{N(A)} + \dots, \quad (5a)$$

$$\frac{1}{x} F_2^{\ell N(A)} = \frac{4}{9} (u_{N(A)} + \bar{u}_{N(A)}) + \frac{1}{9} (d_{N(A)} + \bar{d}_{N(A)}) + \frac{1}{9} (s_{N(A)} + \bar{s}_{N(A)}) + \dots, \quad (5b)$$

Figure 3. QCD mechanism for charge-exchange leading-twist DDIS $\gamma^* p \rightarrow n X^+$.

where $\sigma_A/A\sigma_N \approx F_2^A/AF_2^N$.

Notice that V^0 propagates on-shell. This means that not all the propagators in the graph can be considered as being hard (of order Q^2): this invalidates the OPE, and, as a consequence, the MSR. Most important, the finite path length due to the on-shell propagation of V^0 between N_1 and N_2 contributes to the distance $(\Delta z)^2$ between the two virtual photons in the $\gamma^* A \rightarrow \gamma^* A$ amplitude. One no longer has $(\Delta z)^2 \approx 1/Q^2$. The distance between the currents cannot be less than the inter-nucleon distance, invalidating also the OPE and the parton MSR.

The one-step two-step mechanism describing nuclear shadowing and anti-shadowing explains how parton reinteractions in a nucleus are an essential element in high energy reactions, since they can generate non-trivial contributions at leading twist and thus survive at high Q^2 and high invariant mass, $W^2 = (q + p)^2$. Most importantly, it brings to the forefront the importance of describing deeply virtual scattering phenomena from nuclei at the amplitude level, where the phase structure plays a key role.

In order to test the explanation of anti-shadowing, one could verify the existence of Bjorken-scaling, leading-twist charge exchange DDIS reactions such as $\gamma^* p \rightarrow n X^+$, with a rapidity gap due to an $I = 1$ Reggeon exchange. Here X^+ is the sum of final states with charge $Q = 1$. Since Pomeron exchange does not contribute to the charge exchange process, this would single out Reggeon exchanges as the source of anti-shadowing. This process is shown in Fig. 3. Furthermore, deeply virtual Compton scattering (DVCS) and related experiments on nuclei would display a similar shadowing/anti-shadowing pattern as in the forward DIS limit, enhanced by the extra four-momentum, t , dependence [23].

Note that other classes of DIS processes have been shown to be directly sensitive to the rescattering of the struck quark, for example, the pseudo- T -odd Sivers effect [24, 25]. The “handbag” approximation to DVCS defines the “static” contribution [26, 27] to the measured PDFs, Transverse Momentum Distributions (TMDs), etc. Similarly, nuclear DDIS involves the exchange of gluons after the quark has been struck by the lepton [28]. In each case the corresponding scattering amplitude is not given by the handbag diagram, since interactions between the electroweak currents at different points, $j^\mu(z)$ and $j^\nu(0)$, are essential. The FSI associated with the Sivers effect (“lensing” corrections [24, 29]) survive when both W^2 and Q^2 are large, since the vector gluon couplings grow with energy. However, in this case the final state phase is associated with a Wilson line which, at variance with the nuclear two-step process, produces an augmented Light Front Wave Function (LFWF) [30], that does not affect the x moments, or the sum rules.

Even in the case of the proton, Mueller [31] has noted that the OPE applied to DIS fails at small x_{Bj} . The mechanism is however different: due to the diffusion of gluons to small values of momentum transfer, it is not possible to separate soft and hard scales in this region. This might be related to the fact that at small x there are Fock states with a large number of small x partons, due to processes such as parton fusion and overlapping, which means that the invariant mass of these configurations is undefined. Therefore the usual derivation of sum rules based on the handbag diagram for (forward) double virtual Compton scattering may be inapplicable even on a single nucleon (see detailed discussion in Ref. [32]). In particular, DDIS does not satisfy the OPE nor the MSR. The failure of the OPE and the MSR for DDIS implies that shadowing and antishadowing will not compensate each other to restore the MSR for nuclear structure function. The NuTeV results provide direct evidence for the failure of the MSR for the nuclear structure functions.

In conclusion, we summarize the main results of our paper:

(1) We have illustrated why anti-shadowing of nuclear structure functions is non-universal, *i.e.*, flavor dependent, and why shadowing and anti-shadowing phenomena are incompatible with the standard application of the OPE. As a consequence, sum rules cannot be extracted from nuclear DIS structure functions.

(2) We reiterate that because of the rescattering dynamics, the DDIS amplitude acquires a complex phase from Pomeron and Regge exchange; thus final-state rescattering corrections lead to nontrivial “dynamical” contributions to the measured PDFs, *i.e.*, they are a consequence of the scattering process itself [16, 19, 25, 33]. The $I = 1$ Reggeon contribution to DDIS on the front-face nucleon then leads to flavor dependent anti-shadowing [19, 20]. This could explain why the NuTeV charged current measurement $\mu A \rightarrow \nu X$ scattering does not appear to show anti-shadowing, in contrast to deep inelastic electron-nucleus scattering as discussed in Ref. [9] and illustrated in Fig. 2.

(3) Finally, the Regge exchanges-based theoretical description of shadowing-antishadowing presented here is ideal for realistic, quantitative evaluations of the nuclear structure functions in the upcoming EIC kinematic framework.

Acknowledgments

We are thankful to Simonetta Liuti for her collaboration in earlier stages of this work. This research was supported by the Department of Energy contract DE-AC02-76SF00515 (SJB), by ANID PIA/APOYO AFB180002 (Chile) by FONDECYT (Chile) under Grants No. 1180232 and No. 1191103, and by Millennium Institute for Subatomic Physics at the High-Energy Frontier (SAPHIR) of ANID, Code: ICN2019_044 (Chile). SLAC-PUB-17626.

References

- [1] G. A. Miller and S. J. Brodsky, Phys. Rev. C **102**, 022201 (2020).
- [2] S. J. Brodsky, I. Schmidt, and S. Liuti, [arXiv:1908.06317 [hep-ph]].
- [3] M. Tzanov *et al.* (NuTeV Collaboration), Phys. Rev. D **74**, 012008 (2006).
- [4] J. P. Berge *et al.*, Z. Phys. C **49**, 187 (1991).
- [5] A. C. Benvenuti *et al.* (BCDMS Collaboration), Phys. Lett. B **189**, 483 (1987).
- [6] P. Amaudruz *et al.* (New Muon Collaboration), Nucl. Phys. B **441**, 3 (1995).
- [7] M. Arneodo *et al.* (New Muon Collaboration), Nucl. Phys. B **481**, 3 (1996).
- [8] <https://www.hepdata.net/>
- [9] I. Schienbein, J. Y. Yu, C. Keppel, J. G. Morfin, F. Olness, and J. F. Owens, Phys. Rev. D **77**, 054013 (2008).
- [10] J. Mousseau *et al.* (MINERvA Collaboration), Phys. Rev. D **93**, 071101 (2016).
- [11] B. G. Tice *et al.* (MINERvA Collaboration), Phys. Rev. Lett. **112**, 231801 (2014).
- [12] K. Kovarik, I. Schienbein, F. I. Olness, J. Y. Yu, C. Keppel, J. G. Morfin, J. F. Owens, and T. Stavreva, PoS EPS **HEP2011**, 289 (2011).
- [13] N. Kalantarians, C. Keppel, and M. E. Christy, Phys. Rev. C **96**, 032201 (2017).
- [14] B. Kopeliovich, J. Morfin, and I. Schmidt, Prog. Part. Nucl. Phys. **68**, 314 (2013).
- [15] N. N. Nikolaev and V. I. Zakharov, Phys. Lett. **55B**, 397 (1975).
- [16] L. Stodolsky, Phys. Lett. B **325**, 505 (1994).
- [17] M. Derrick *et al.* (ZEUS Collaboration), Phys. Lett. B **315**, 481 (1993).
- [18] T. Ahmed *et al.* (H1 Collaboration), Nucl. Phys. B **429**, 477 (1994).
- [19] S. J. Brodsky and H. J. Lu, Phys. Rev. Lett. **64**, 1342 (1990).
- [20] S. J. Brodsky, I. Schmidt, and J. J. Yang, Phys. Rev. D **70**, 116003 (2004).
- [21] L. A. Harland-Lang, A. D. Martin, P. Motylinski, and R. S. Thorne, Eur. Phys. J. C **75**, 204 (2015).
- [22] S. Alekhin, J. Blümlein, S. Moch, and R. Placakyte, Phys. Rev. D **94**, 114038 (2016).
- [23] S. Liuti and S. K. Taneja, Phys. Rev. C **72**, 032201 (2005).
- [24] S. J. Brodsky, D. S. Hwang, and I. Schmidt, Phys. Lett. B **530**, 99 (2002).
- [25] S. J. Brodsky, D. S. Hwang, Y. V. Kovchegov, I. Schmidt, and M. D. Sievert, Phys. Rev. D **88**, 014032 (2013).
- [26] S. J. Brodsky, AIP Conf. Proc. **1105**, 315 (2009).
- [27] S. J. Brodsky, Nucl. Phys. A **827**, 327C (2009).
- [28] S. J. Brodsky, P. Hoyer, N. Marchal, S. Peigne, and F. Sannino, Phys. Rev. D **65**, 114025 (2002).
- [29] M. Burkardt, Nucl. Phys. A **735**, 185 (2004).
- [30] S. J. Brodsky, B. Pasquini, B. W. Xiao, and F. Yuan, Phys. Lett. B **687**, 327 (2010).
- [31] A. H. Mueller, Phys. Lett. B **396**, 251 (1997).
- [32] S. J. Brodsky, V. E. Lyubovitskij, and I. Schmidt, [arXiv:2105.01435 [hep-ph]].
- [33] T. H. Bauer, R. D. Spital, D. R. Yennie, and F. M. Pipkin, Rev. Mod. Phys. **50**, 261 (1978); **51**, 407(E) (1979).